CHAPTER 7

Interpretations and Theoretical Models

In our sample there is a large number of Mira variables from which we have not detected SiO maser emission. In the first part of this chapter we discuss the possible reasons for these non-detections. In the second part, we attempt to arrive at an overall picture of the SiO maser phenomenon as suggested by both previous investigations and ours. From several independent considerations, we show that the most likely pump mechanism for the SiO maser is radiative with an essential contribution from the circumstellar dust shell at least for strong SiO masers. Finally, we summarize the conclusions of this thesis.

7.1 Non-detections

Table 1 is an extended version of Table 6.2, with four more columns. We see that there are several Mira variables in the range of spectral-types M6—M10, for which we have only upper-limits on the SiO maser luminosity. These limits are comparable to the luminosities for the masing sources detected in our sample. This raises the question — Why are these Mira variables such weak masers if at all they are masing? In Table 1, we find that there are many sources which have been detected previously, at 43 and 86 GHz. These sources are marked by 'a' and 'b' respectively, in column 7. Generally, the 43 GHz emission is expected to be about twice as strong as the 86 GHz (Snyder and Buhl, 1977). Therefore, those sources which are already weak at 43 GHz should be even weaker at 86 GHz and thus will not be detectable with our sensitivity. On the other hand, there are many sources previously detected at 86 GHz, which we failed to detect. This is most likely due to the fact that all these sources, except R Com, were close to their minimum phases (0.5 to 0.9), as can be seen from Table 1.

Table 1: Non-detections with spectral-type M6.

Source	Phase	SP.Type	M_{bol}	SiO Lum. ($\times 10^{44}$)	Ampl.	Prev. Det.
Ari U	0.74	6.75	-5.13	0.21	8	a
Aur U	0.84	8	-5.23	0.09	8	a,b
Cas Y	0.68	7.25	-5.24	0.16	6.6	a,b
Cen RT	0.4	6.75	-4.73	0.49	5.5	
Cen V744	0.91	8	-3.63	0.01	1.4	
Cep T	0.85	7.15	-5.18	0.02	6.1	a,b
Cnc W	0.33	7.75	-5.19	0.13	7	a
Com R	0.23	6.5	-5.11	0.35	7.5	a,b
Crt S		6.5	-4.21	0.03	1.6	
Crv R	0.95	6.75	-4.96	0.21	7.7	
Cyg Z	0.15	7	-4.77	0.29	7	a,-b
Eri W	0.39	8	-5.15	0.3	7	
Her RU	0.52	7.35	-5.41	0.11	7.5	a,b
Hya RT		7	-4.87	0.04	3.2	
Lib FS	0.41	8.55	-5.25	0.48	5	
Lup R	0.26	6.75	-4.65	0.65	4.6	
Lyr RW	0.67	7	-5.45	0.38	6.2	b
Ori DT	0.71	10	-5.28	0.68	6.6	
Ori S	0.92	8	-5.24	0.04	6.8	a,b
Ser WX	0.64	8	-5.27	1.05	4	a,b
Tau R	0.21	7	-4.98	0.09	8.2	a
Vir BK	0.48	7	-4.17	0.01	1.3	

a: **detection at 43 GHz**
b: detection at 86 GHz
c: non-detection at 86 GHz

The non-detection of W Cnc, Z Cyg and R Tau is surprising. Note that Z Cyg has also not been detected at 86 GHz in a previous observation (Engels and Heske 1989). Their non-detections cannot be attributed to large distances as their upper limits on luminosity are lower than the luminosities of several detected sources. Moreover, they were all close to the maximum in phase. We note that their amplitudes of pulsation in visual magnitudes are large ($\geq$ 7 magnitudes). From Table 1, we also note that except for FS Lib and RT Hya, all other non-detections have large values of pulsational amplitude. This supports

the anticorrelation discussed in Chapter 6.

Returning to Table 1, we notice that the maser non-detections in sources not observed before, have values of $M_{bol} > -4.8$. As seen in Chapters6, maser emission seems to be absent for sources with bolometric magnitudes fainter than this value. These sources are RT Cen, V744 Cen, S Crt and BK Vir.

To summarize this section, there seem to be three criteria which may inhibit a Mira variable from giving rise to SiO maser emission at 86 GHz: They are,

- Spectral-type less than M6 (or $\log T_{eff} \geq 3.48$).
- Bolometric magnitude fainter than -4.8 magnitudes.
- Amplitude of pulsation greater than 6 visual magnitudes.

7.2 Interpretations

7.2.1 Dependence of maser-power on spectral-type

The SiO maser power clearly must depend on the molecular abundance of SiO in the atmosphere of the Mira variable. As seen earlier, one of the main results that has emerged from our observations is that the masing Mira variables have spectral-types later than M6. Indeed, this dependence of the maser power on the spectral type could simply be due to a lower abundance of SiO in stars having spectral-types earlier than M6. Such an abundance variation was in fact predicted by Johnson et al. (1965). Rinsland and Wing (1982)' observed the vibrational-rotational transitions in SiO, at 4μ from several M-giants and a few Mira variables of various spectral-types. They found that the equivalent width of the absorption band increased with the spectral-type. Fig. 1 is adapted from

'We are grateful to T. Tsuji for this reference.

their paper and shows that beyond a temperature of $\sim$ 3000 K, there is a steep decline in the value of the equivalent width. A similar effect is expected also for the abundance of water (Tsuji 1978). We therefore propose a reduction in the abundance of SiO in earlier spectral-types as an explanation of the observed depe.dence of the SiO maser power on effective temperature (spectral-type). This can be tested by future observations of SiO in th rmal rotational transitions from Mira variables covering a wide range of spectral-types.

7.2.2 Correlation of maser-power with bolometric magnitude

The correlation of SiO maser photon luminosity with the bolometric magnitude is consistent with the idea that SiO masers are pumped radiatively. Such a correlation was found earlier also by Cahn and Elitzur (1979) who also proposed a radiative pump. Compared to them, we have twice as many objects, including strong maser emitters as well as non-masing sources. For the bolometric luminosity, we have used the more recently obtained period-luminosity relation which has a very small scatter and is icdependent of the effective temperature, radius and distance. The SiO luminosity shows a correlation with the bolometric magnitude which is expected if the pump is radiative. In addition, we also find a cut-off in bolometric magnitude. For this cut-off value, we later derive the photon luminosity available from the star and show that it is less than the weakest observed maser photon-luminosity. We also show below that the strong masing soruces (which were omitted in the analysis by Cahn and Elitzur) can be explained by including also the IR photons from the dust for the radiative pump. In fact, the scatter seen in our plot (Fig. 6.9) may partly be due, as pointed out by Cahn and Elitzur, to the differences in the properties of dust-grains in

different sources.

7.2.3. Anticorrelation of the maser-power with the amplitude of pulsation

The amplitude of pulsation is larger in visual magnitude than in the infra-red, typically by about 4 to 5 magnitudes. The main reason for this effect may simply be due to the nature of the Planck-curve, the difference between two of which correspond to the typical temperatures at the maximum and minimum, have been plotted in Fig. **2.** It seems therefore possible that the large visual amplitude is simply a measurement of a change in the temperature of the star as it pulsates. In Fig. **3** we plot the ratio of the maser flux to the SiO thermal (v=0) flux now as a function of the amplitude in temperature, calculated from the range of spectral-types given by Lockwood (1972), as discussed in Chapter 6. The trend of anti-correlation is not very clear in this figure. More observatioris of v=0 and v=1 SiO lines using the same telescope to avoid relative calibration uncertainties, will help to resolve this uncertainty, Even so, it appears that temperature changes do not play a major role in maser emission.

An additional reason for the large difference in the amplitudes at visual and infra-red wavelengths has been suggested by Bertschinger and Chevalier (1985) *viz.* an enhanced luminosity in the visual region due to the onset of shocks at the maximum phases during pulsation. Although this theoretical work does not study the strength of the shocks as a function of the amplitude of pulsation, it seems reasonable to expect stronger shocks for larger amplitudes of pulsation. Qualitatively, this may provide an explanation for the anti-correlation seen between the maser emission and the amplitude of pulsation because a strong shock would disturb the velocity coherence which is required in the medium

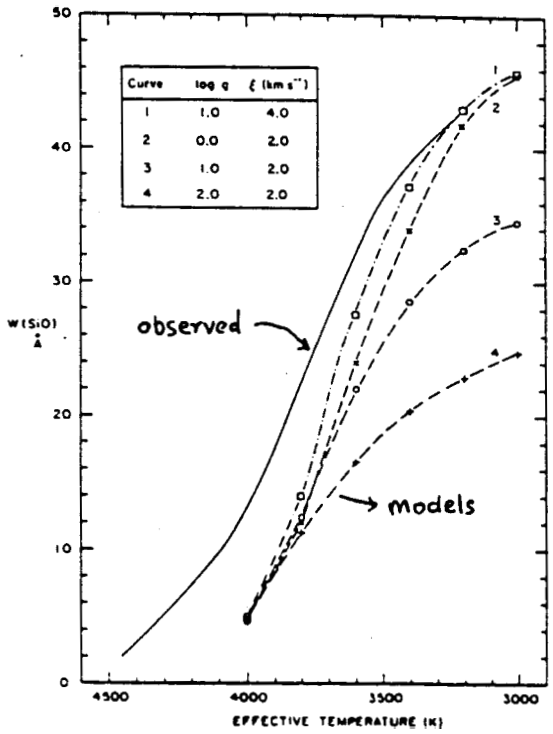

Figure 1: Dependence of abundance of SiO on the effective temperature. (Adapted from Rinsland and Wing, 1982)

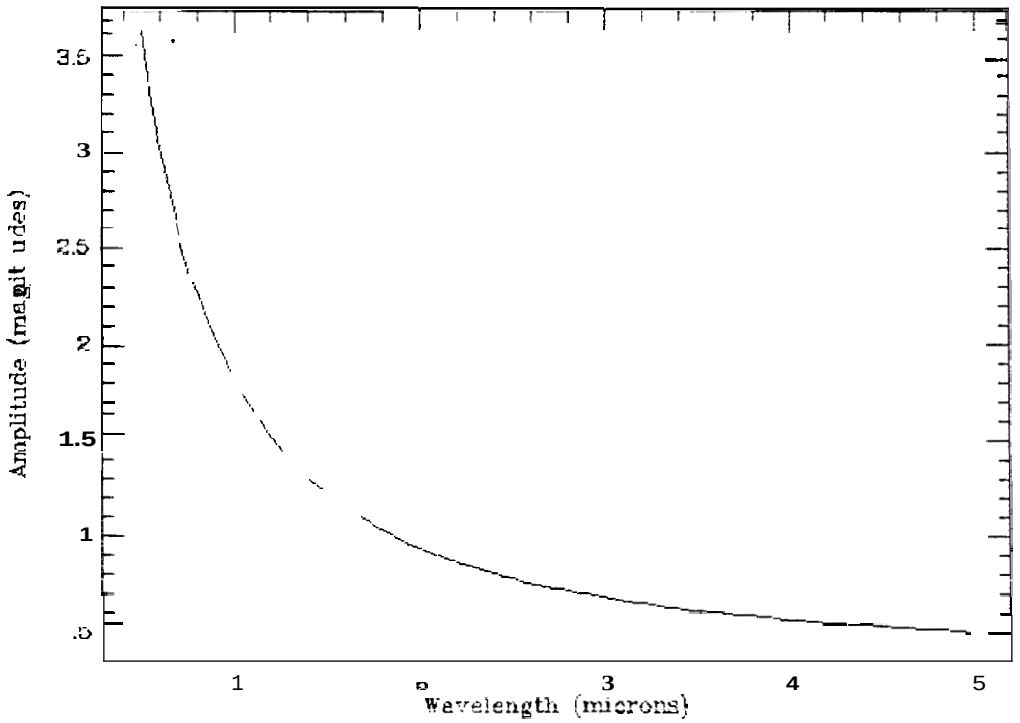

Figure 2: This figure shows that Am, $< \Delta m_{IR}$ for a given change in temperature of a black-body

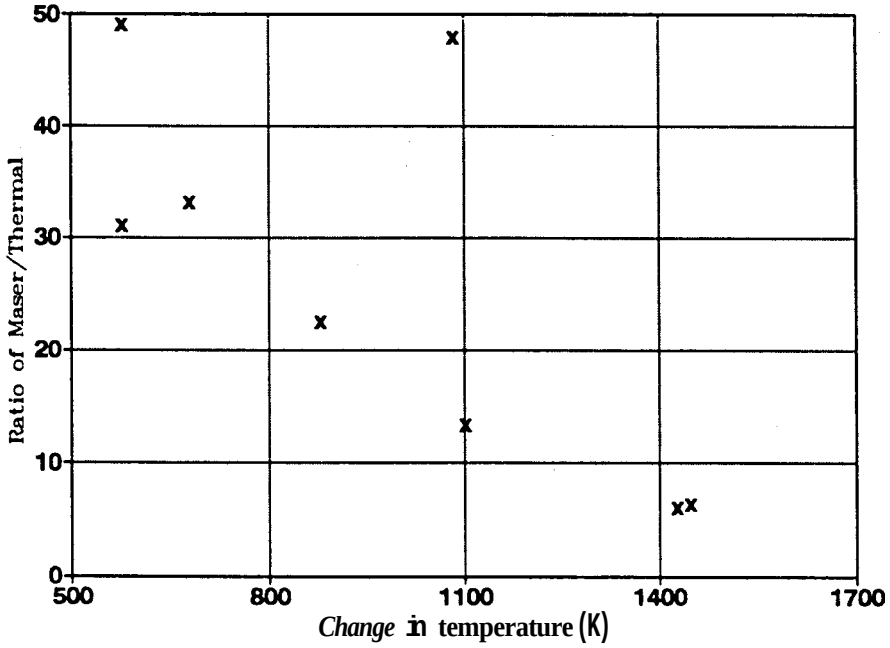

Figure 3: To check for the correlation with the range of temperature changes

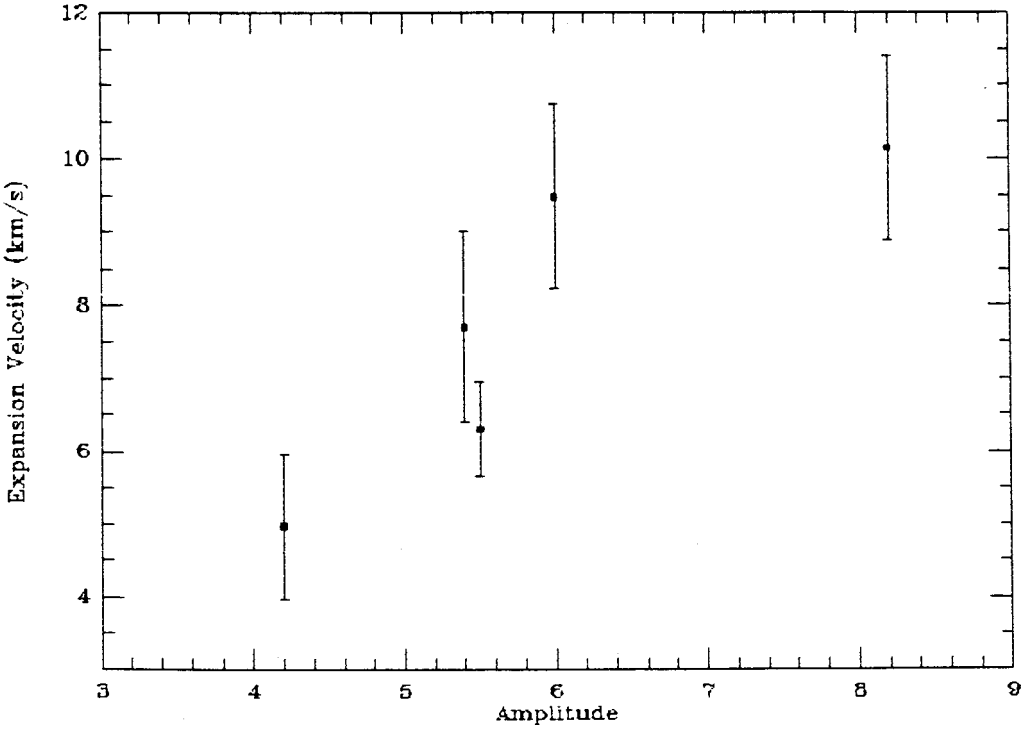

Figure 4: Correlation between the expansion velocity and the amplitude of pulsation.

for the amplification of the SiO emission. Hinkle et al. (1982) have observed the vibrational-rotational transitions in CO, occuring near 2μ. Based on these observations, they point out that the shock phenomenon will give rise to more radical changes in the maser emission than what one observes; implying that the SiO masers cannot reside as close to the photosphere as was suggested earlier. (It is in this region that the observed infra-red CO emission originates). If the masing region is radially further out, where the steady outflow of matter dominates and not the shocks, it would be important to check for the effect of the outflow velocity on the maser emission. Hinkle et al. provide a table of expansion velocities obtained from SiO and CO observations. In Fig. 4, we find a correlation between the expansion velocity and the amplitude of pulsation. This figure provides a possible explanation for the anti-correlation between the maser power and the amplitude of pulsation. A larger amplitude implies a larger expansion velocity and since the extent of the masing region is less likely to vary by a large factor, an increase in the expansion velocity causes a corresponding increase in the velocity gradient. Due to the velocity gradient, the available physical path-length is given by,

$$\Delta x = \frac{\Delta V_{thermal}}{\frac{\partial v}{\partial r}}, \qquad (1)$$

where $\Delta V_{thermal}$ is the thermal line-width in terms of velocity. For a saturated maser, the power is propotional to the optical depth in the line and thus, this coherence length **Ax** will be smaller for a larger velocity gradient giving rise to a weaker maser.

7.2.4 High angular resolution observations

VLBI observations of SiO masers around late-type stars have been made by Moran et al. (1979), Lane et al. (1984) and McIntosh et al. (1989). Orion has been observed at high angular resolution by Genzel et al. (1979) and Plambeck et al. (1989). An important recent study on the spatial distribution of SiO maser emission from R Cas was done by McIntosh et al. (1989). The main results found by them are:

- The circumstellar environment is clumpy as traced by the SiO maser.
- The strongest emission in the line-profile has the weakest polarization.
- The pattern of masing spots seems to have changed with time.

This work reveals for the first time the variation of the spatial locations of masing spots if one compares their map in Fig. 5, with the map in Fig. 6, of the same source, observed 7 years earlier by Lane et al. (1979). In both these maps, there appears to be an elongated distribution of emission features. In 1979, the emission was extended along an axis having a position angle of 110 degrees E of N. The present data shows an elongation axis of 20 degrees, i.e., it is perpendicular to the earlier orientation. More observations are clearly needed to unravel the kinematics of the SiO masing spots.

In the line-profile from R Cas, observed by McIntosh et al., there are two strong features, the strengths of which depend on the pulsation phase. The variation in the strength of one feature follows that of the other, with a time lag of about 10 days. These spots are separated on the sky, by about 10^{14} cm. McIntosh et al. use this fact to provide a constraint on the pump mechanism by

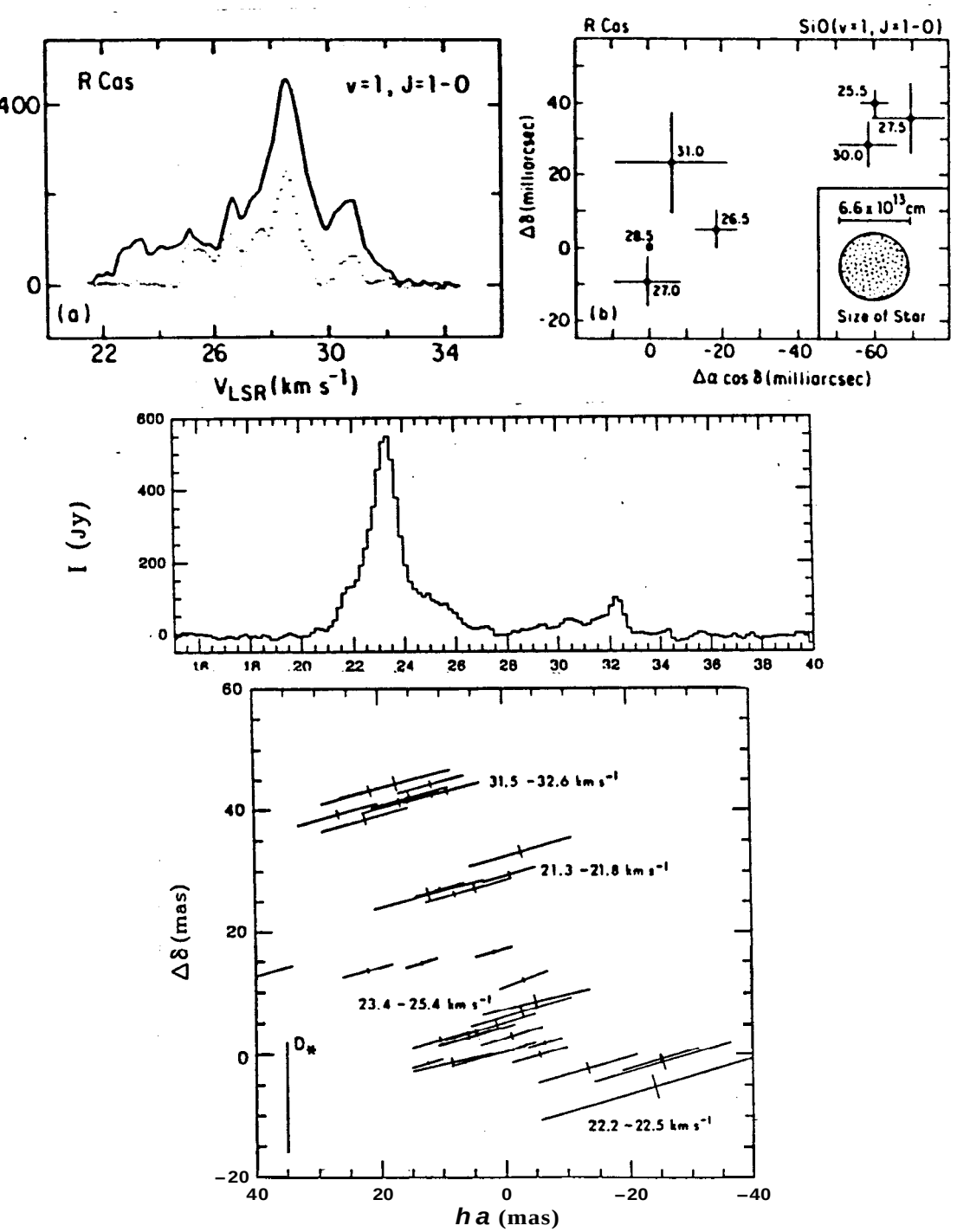

Figure 5: Variation of the spatial location of masing spots in R Cas, over a period of 7 years. Taken from Lane et al. (1979) and McIntosh et al. (1989)

saying that any pump mechanism should be able to propagate over this distance within a maximum time interval of $\sim$ 10 days, i.e., a speed of $\geq 10^8$ cm/sec. They suggest therefore, that the most likely pumping mechanism is radiative and not hydrodynamic or MHD shocks. However, we note that this lower limit on the speed of the pump mechanism, is valid **only** if the projected distance represents also the distance along which the pump mechanism propagates. Thus, their argument does not conclusively indicate a radiative pump.

In their observations, we also see an indication that the stronger emission fades out slower than the weaker. If true, then the weaker features may correspond to unsaturated maser emission, while the strong emission may be saturated.

From the existing VLBI observations (McIntosh et al. 1989, Lane et al. 1984, Moran et al. 1979) we get the observed spread of the masing spots in R Cas to be within a diameter of 0."04 to 0."07. The star's angular diameter is about 0."02 (ref). However, the star's position in the VLBI map is not known to an accuracy better than 0."3 (Wright et al. 1990). If we assume a symmetrical distribution of the masing spots around the location of the star then we get a mean distance of about $4R_*$, where R_* is the radius of the star. We assume here that the distribution of the masing spots around R Cas is typical. Only a few VLBI observations are available, but all sources show a similar angular spread of the masing spots. Note that in supergiants however, the masing spots may be spread over a larger distance (e.g., 5–7 R_* for VX Sgr).

Later, we shall use this average distance of the maser spots from the star, to obtain the physical characteristics of the region where the masing occurs.

7.2.5 Variability of the maser emission

Previous studies of time-variation of the SiO maser emission have concentrated mainly on checking whether the variation of the integrated maser flux is correlated with the variation of the light from the star as it pulsates. In this section, we discuss this correlation, including the variation of the effective temperature of the star. Among the sources which have been observed at near infra-red wavelengths, some have also been extensively monitored in the SiO maser emission (Martinez et al. 1989, Nyman 1984). The latter authors have found good correlation between the variation of the SiO maser and 1.04 μ fluxes. Martinez et al. (1989)'s observations are the most extensive so far. They have studied the variation of the maser flux with respect to the phase of pulsation and for o Cet and U Her, they also plot the optical light curve along with the maser light curve. We have selected five such sources: o Cet, R Cas, U Her, R Leo and R LMi and plotted against the pulsation phase, their available SiO maser fluxes, 1.04 micron magnitudes, visual magnitudes and effective temperatures in Fig. 6. From these figures one can calculate the mean values of phases at maxima and minima for the light-curves. They are as follows:

Source	Visual		IR		Temperature		Maser	
	max	min	max	min	max	min	max	min
o Cet	0	0.6	0.17	0.65	0.15	0.65	0.2	0.75
R Cas	0	0.57	0.1	0.6	0	0.55	0.1	0.55
U Her	0	0.57	0	0.58	0	0.6	0.05	0.55
R Leo	0	0.55	0	0.55	0	0.65	0.2	0.5
R LMi	0	0.6	0.1	0.5	0.1	0.5	0.1	0.5

The maser flux variation lags with respect to the optical, by about 0.1 to 0.2. This phase lag is seen also in the infra-red light-curves and in the temperature variations. However, for one source, i.e., R Hya the infra-red maximum precedes

the optical one. It will be useful to include this object in future time-monitoring programs of SiO observations, to find out if the maser emission too leads the optical for this source.

All these sources show a very regular behaviour in the 1μ magnitude. On the other hand, in different cycles, the maser flux values at a given phase often differ with each other by as much as a factor of **2.** There exists a similar irregularity over different cycles in values of effective temperatures. The relatively most regular variation in maser emission is seen in o Cet which also shows a regular variation in the temperature. But, unless one monitors both the maser and the temperature in the same cycle of pulsation, one cannot learn about a physical relation between these two quantities.

The phase lag in the IR light-curves with respect to the visual light-curve, is a function of wavelength. Starting from the visual light-curves, as seen in Fig. 7, upto the wavelength of $\sim 1\mu$, there is a steady increase of the phase lag which reaches a value of $0.1 \sim 0.2$. Fig. 8 is from Harvey et al. (1974), and it shows that from 1μ to 10μ, there is no further increase of the phase-lag with respect to the visual light-curve. The SiO maser variation also has a phase-lag of a similar amount as discussed earlier. It is possible that the light-curves for wavelengths smaller than 1μ have a phase lead due to a transient event. Bertschinger and Chevalier (1985) show that this transient event could be due to the pulsational shock. This shock may dissociate the molecules close to the photosphere, hence unveiling an optical blanket and enhancing the visual light at 0 phase. The infra-red is therefore the true indicator of stellar pulsational phase and not the visual light. Since the maser agrees in phase with the infra-red, it points towards the pumping being radiative.

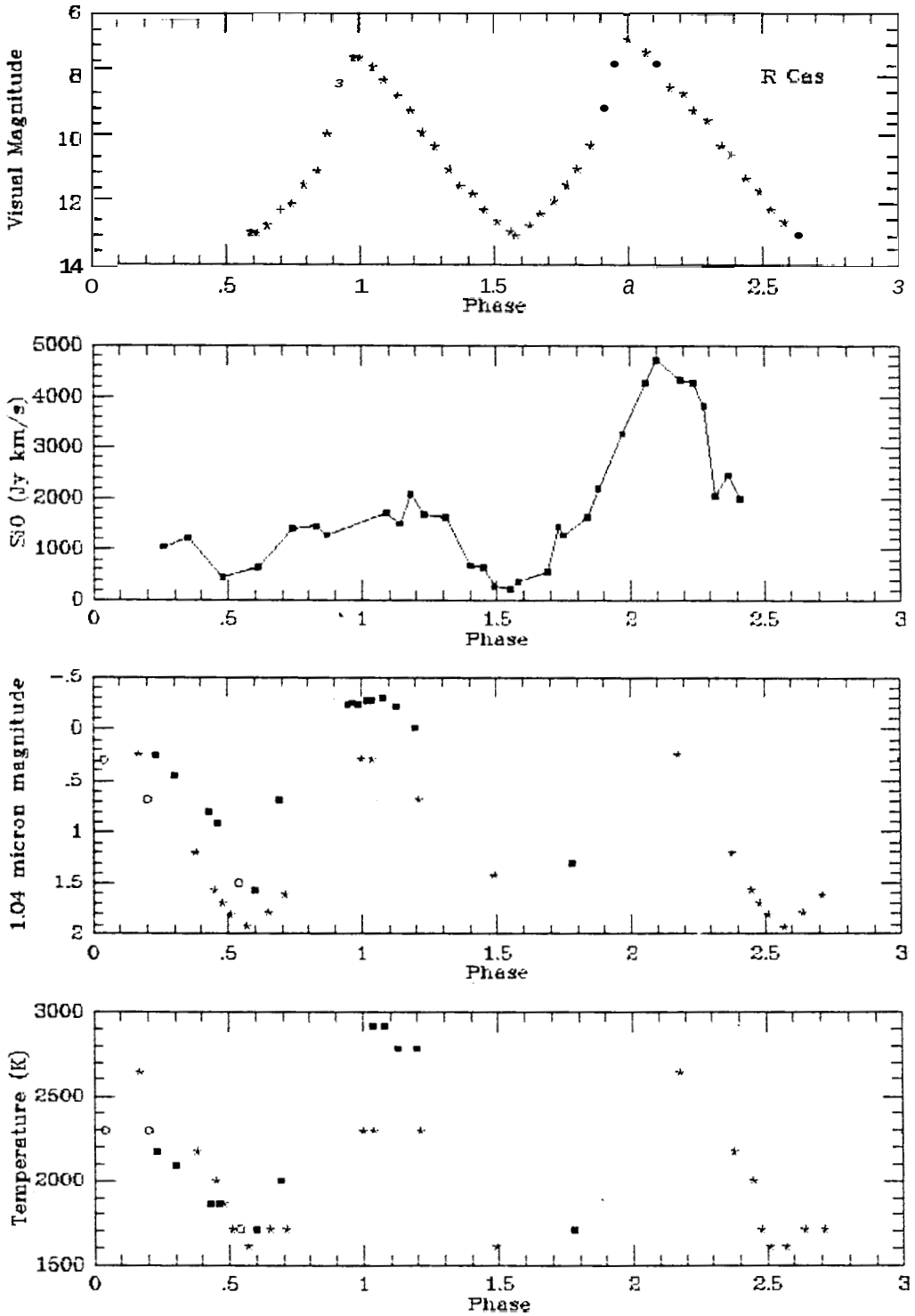

Figure 6: Time variations of SiO maser flux, visual and IR magnitudes and temperature. Different symbols represent data from different cycles of pulsation

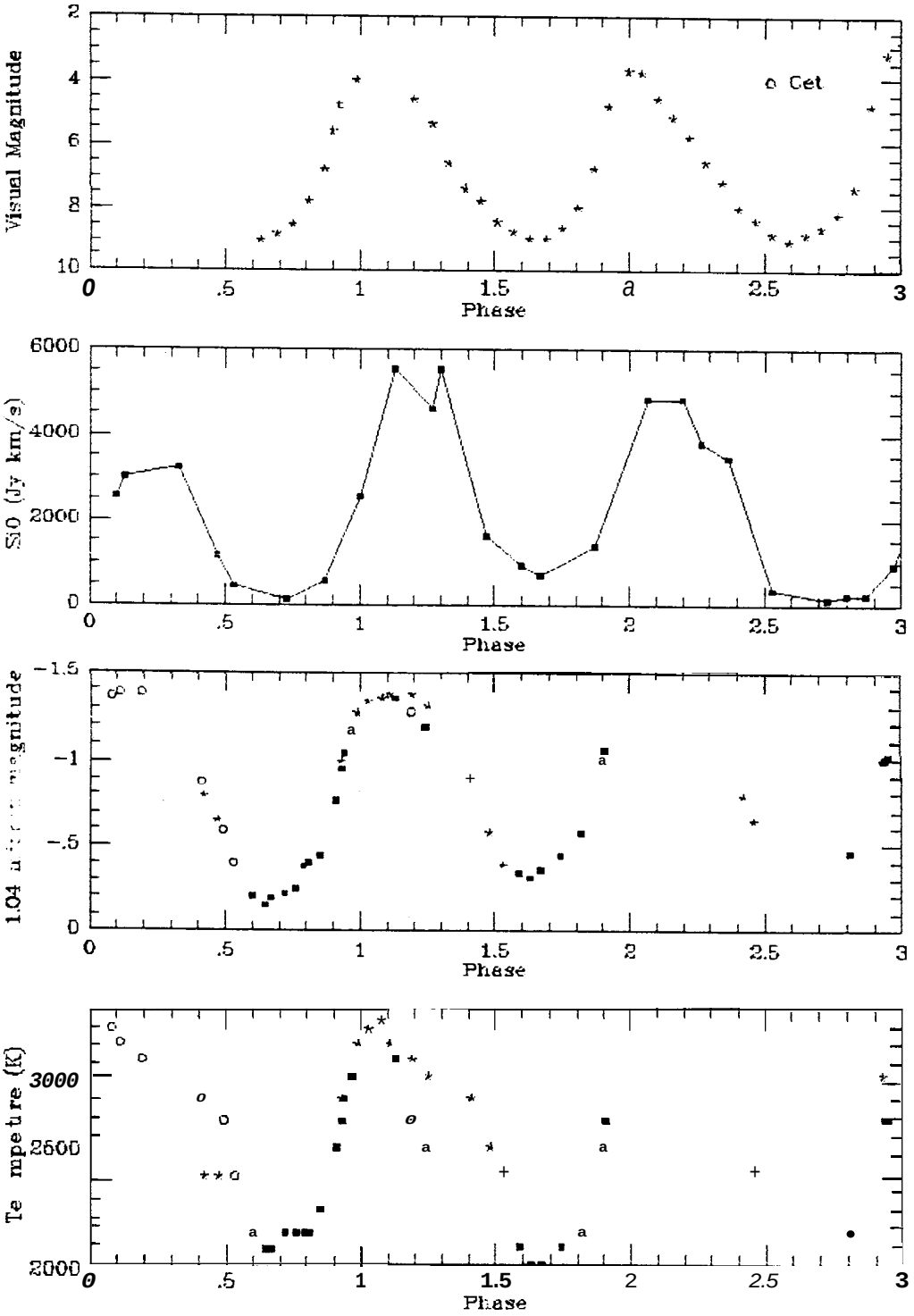

Figure 6: (contd.)

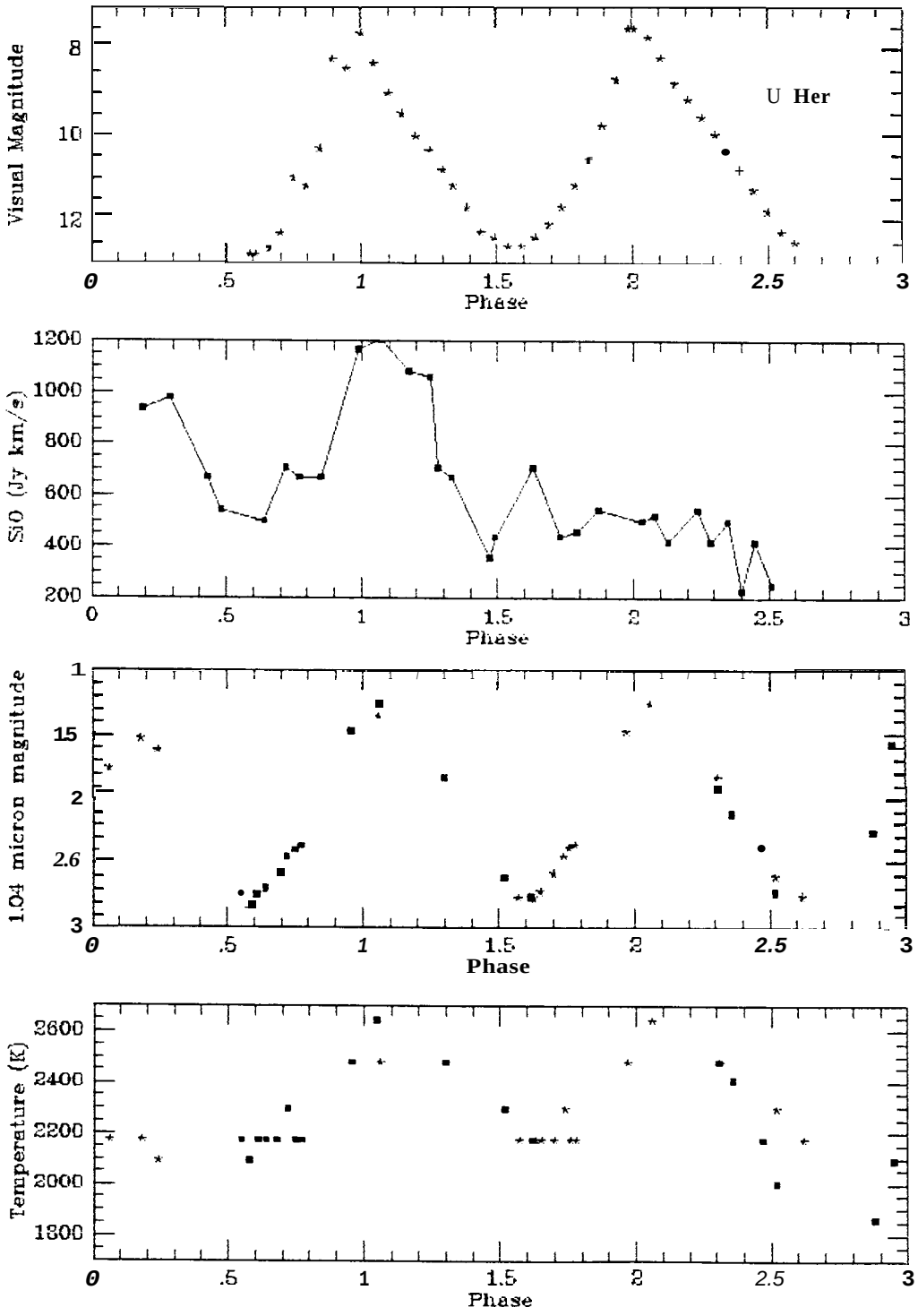

Figure 6: (contd.)

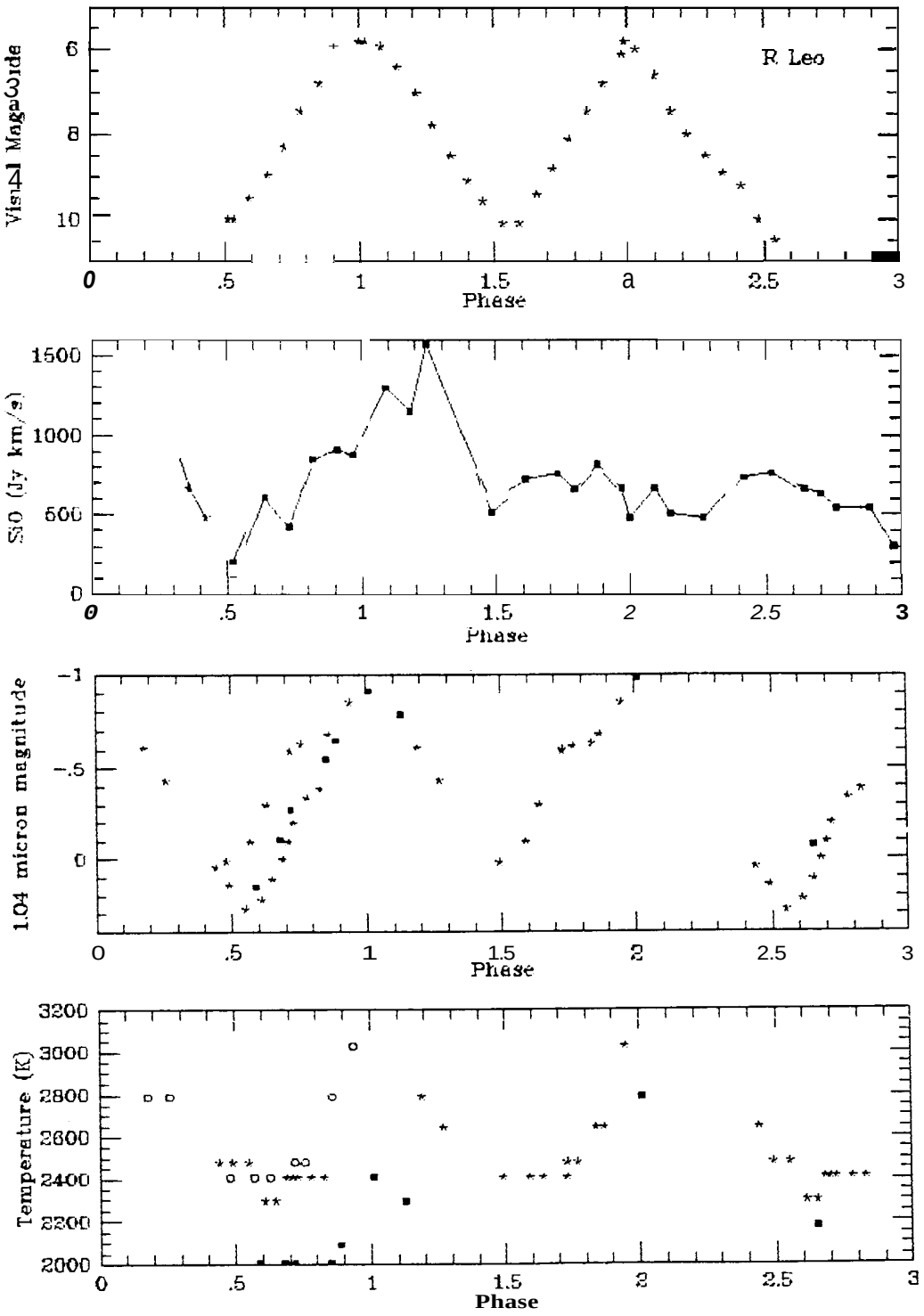

Figure 6: (contd.)

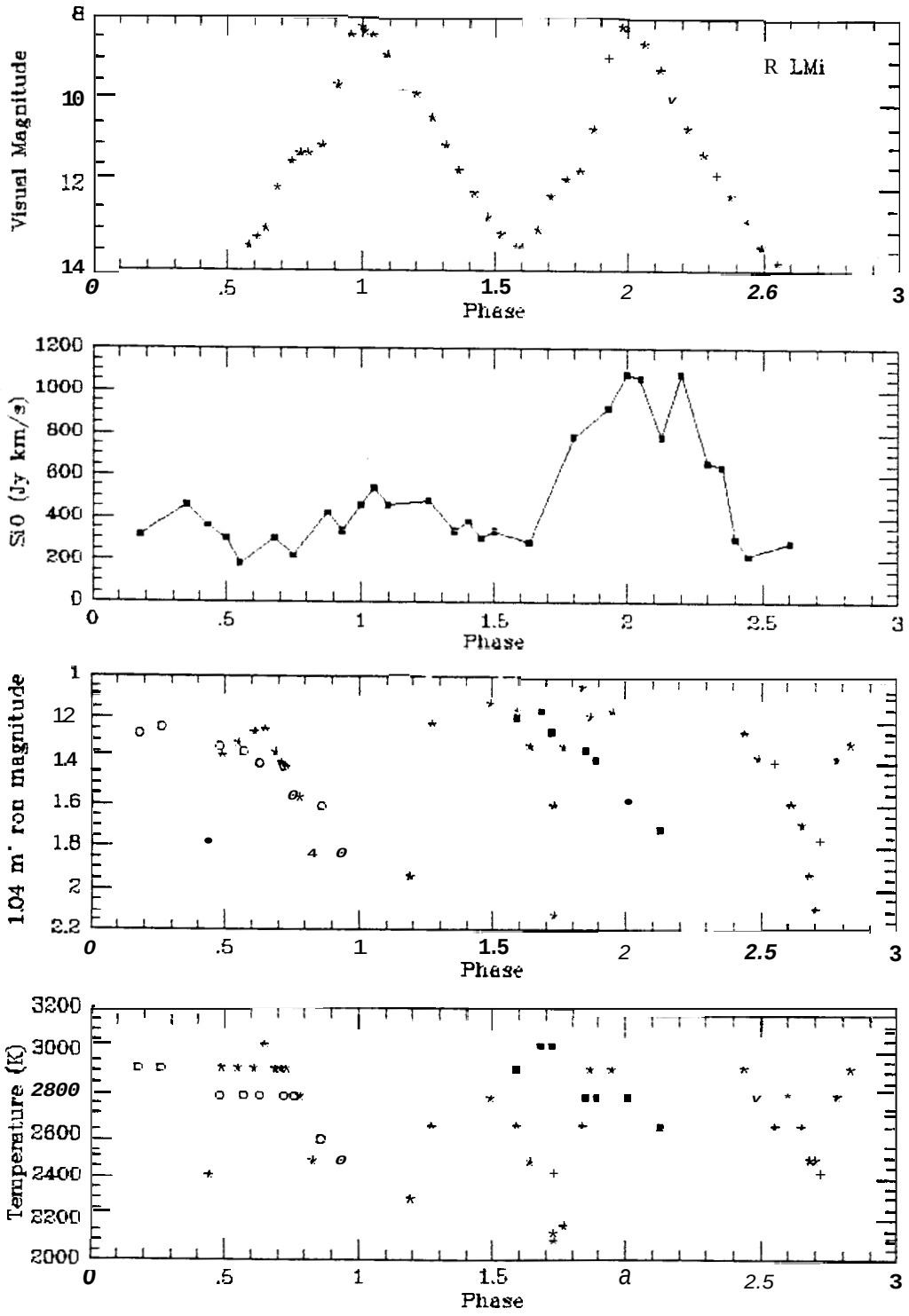

Figure 6: (contd.)

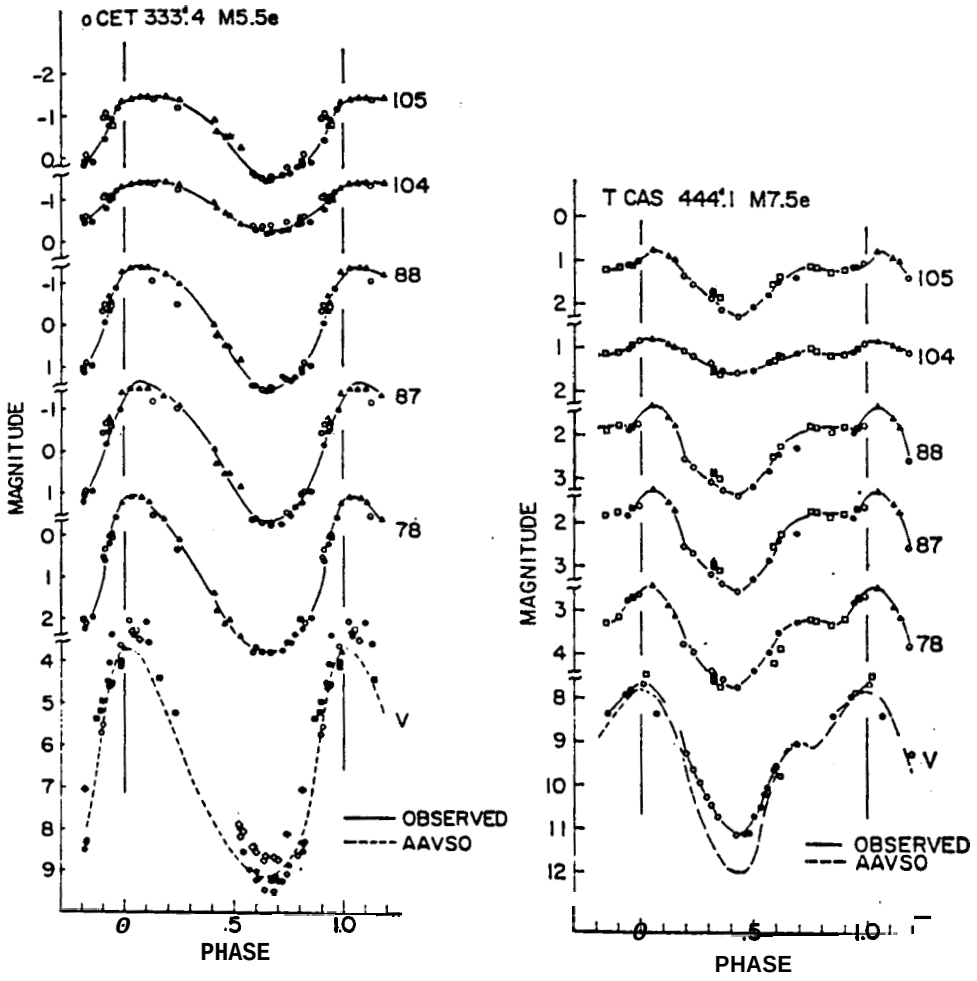

Figure 7: Mira light-curves at different IR wavelengths

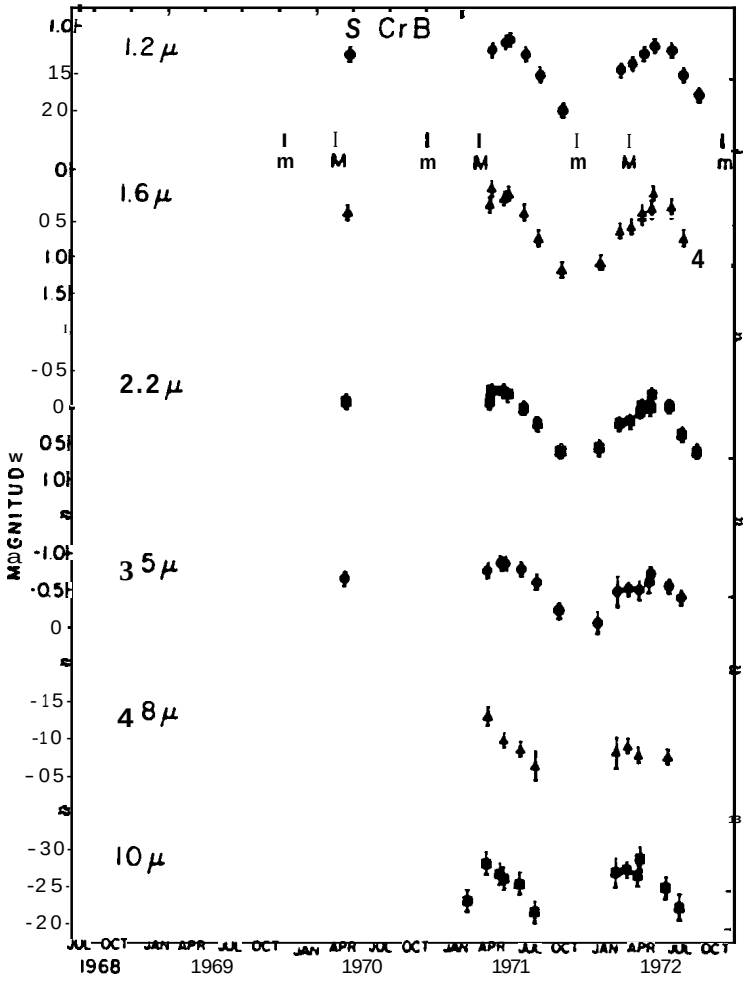

Figure 8: Constant phase for wavelengths beyond 1μ

Time variation of maser emission from Orion

In Chapter **3,** we have seen that there is a systematic change in the flux of maser emission from Orion, over a time-scale of a few months. Orion has been monitored previously, by Hjalmarson and Olofsson (1979), Nyman (1984) and Martinez (1989). We note from Hjalmarson and Olofsson's observations that the negative velocity feature shows large and smooth variations in the flux by about 50 to 100%, over a time scale of about 14 months, while the positive velocity feature does not vary by more that about $\sim$ 30% during this period. The time-variation of peak fluxes of the blue-shifted and red-shifted features is plotted in Fig. 9, using the observations of Hjalmarson and Olofsson (1979) and Nyman (1984). The variations in Orion emission seen by us (Fig. **3.2)** are consistent with these. Due to its variability Orion is not a suitable calibration source.

Short term time/polarization variations

So far, all the time-monitoring observational programs have made observations spaced over intervals of a few weeks. Compared to the period of pulsation, this still provides enough sampling to infer the relation between maser flux changes and the stellar-pulsation. However, since the SiO maser is often believed to be located close to the photosphere where the dynamics of the gas is complicated, one must check for time-variation of the maser emission, over time-scales much shorter than the pulsational time-scale. We have attempted such a monitoring on R Leo and observed variations in the velocities and intensities of the maser features over a time-scale of the order of **2—3** days. Figs. 10 show that there are significant changes in the profile over such short time intervals. The difficulty in our observations which hinders detailed interpretation at this stage, is that

some of this variation is also likely to be due to different polarizations within the line-profile, and the fact that our observations were made at arbitrary hour-angles, with a linearly polarized feed. The values of the polarization parallactic angles are indicated along the spectra in Figs. 10. The antenna temperature of the two main components in this line-profile shows a variation as a function of the parallactic angle. This variation is shown in Fig. 11. One can infer from this figure that the weaker component is more strongly polarized than the more intense feature, which is in agreement with the observation of McIntosh et al. (1989) for R Cas, and also of Clark et al. (1979) for R Leo discussed earlier. The changes seen in the profiles acquired on different days could also be due to inherent variations in the source. Previous investigators have often found indications of such short-term variations in both intensity and polarization from W Hya and R Cas (Troland et al. 1979, Allen 1984). More observations which seperate out the effect of polarization, and spaced over an interval of few hours, are needed to investigate these intensity changes in detail.

Long-term velocity variation: Is the maser emission arising from surviving Jovian-like planets?

Curtis Struck-Marcell (1988), has proposed a hypothesis based on the existing characteristics of the SiO maser emission and a detailed model of the atmosphere of Mira variables, that the source of SiO required for the maser, could be evaporation of the satellites of Jovian-like planets around the evolved star. He has shown that the evaporated matter from the satellites is not likely to escape the gravity of the planets, and suggested that it is the SiO in this gas that is masing. This interesting idea can be checked only by very long-term time-monitoring of

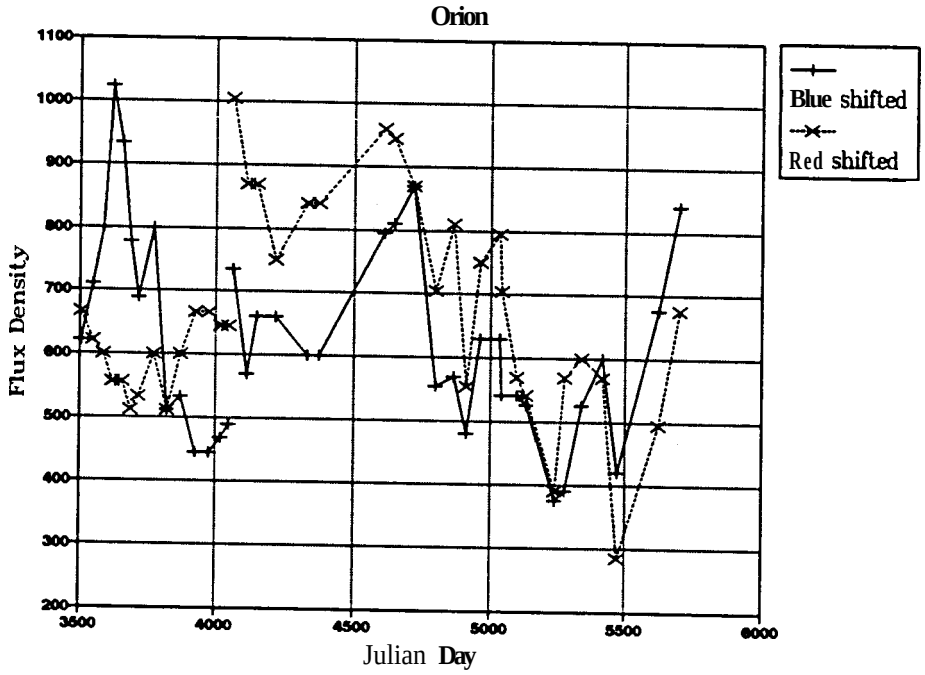

Figure 9: Orion: long-term time-variations

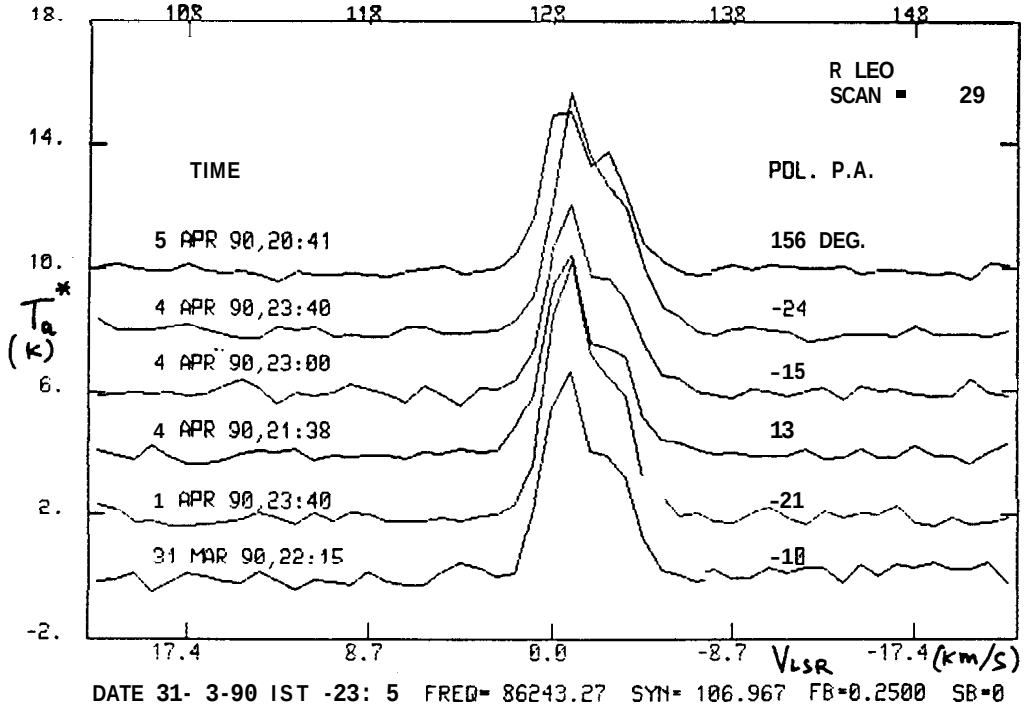

Figure 10: R Leo: Short-term time/polarization variations

the masing spots, as the orbital time-scale for such planets is expected to be of the order of 10 years. Although VLBI time-monitoring has not been done so far, single-dish observations do exist for some strong sources over a time scale of at least 5 years. For R Leo, we have attempted to compile the velocity of the strongest feature in the profile from all the available observations. The variation of the velocity is shown in Fig. 12. The data in this plot is obtained from Hjalmarson and Oloffson (1979), and Nyman (1984). From this figure one sees that the behaviour of the velocity is far more complicated than a regular variation one expects from a body revolving around the star. The planetary model therefore appears to be too simple to incorporate these complicated changes in the velocity.

7.2.6 Maser emission from higher vibrational states

SiO maser emission has been observed in vibrational levels going upto v=3. The energy difference between one vibrational state to the next corresponds to a temperature of about 1800 K. Since the higher v states probably probe the hotter regions, nearer to the photosphere, it is useful to compare the maser emission arising from different v states. Allen (1984) presents simultaneous observations of J=1—0 transitions, in v=1,2 and 3, from many sources. He finds an interesting result that there is an increase in the average emission velocity with higher vibrational state. This is contrary to what one expects if the average acceleration of matter is always radially outward, and thus the v=2 and v=3 emission is likely to be from infalling matter. A similar study made later by Alcolea et al. (1989), does not show this difference in velocity as a function of v-state. However, the velocity resolution in Alcolea et al.'s observations is 0.35 km/s whereas Allen (1984)'s observations were made with a resolution of

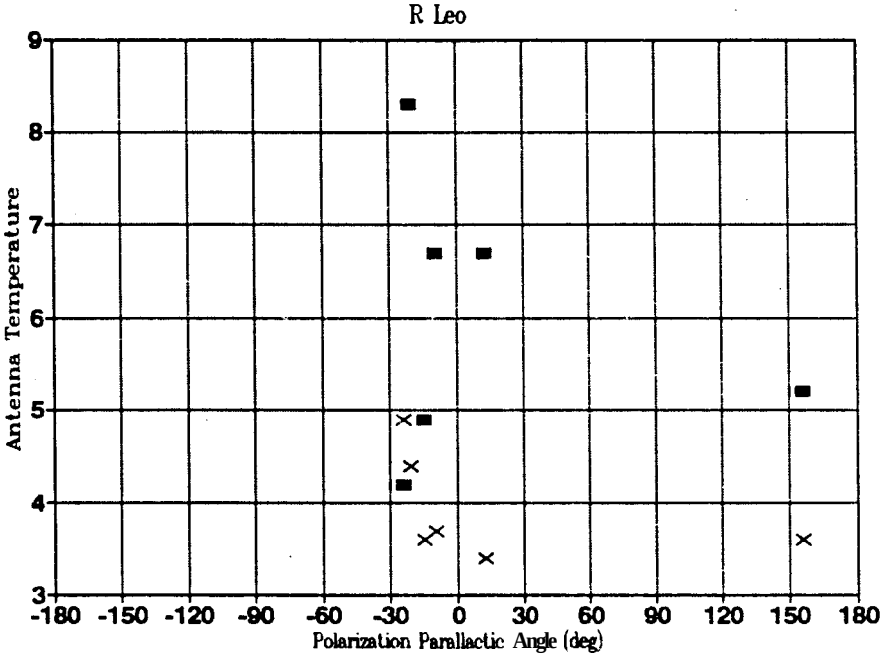

Figure 11: R Leo: Polarization differences in the profile. The weaker feature is shown by a 'x'. It shows a more regular behaviour compared to that of the stronger feature, with respect to the polarization parallactic angle.

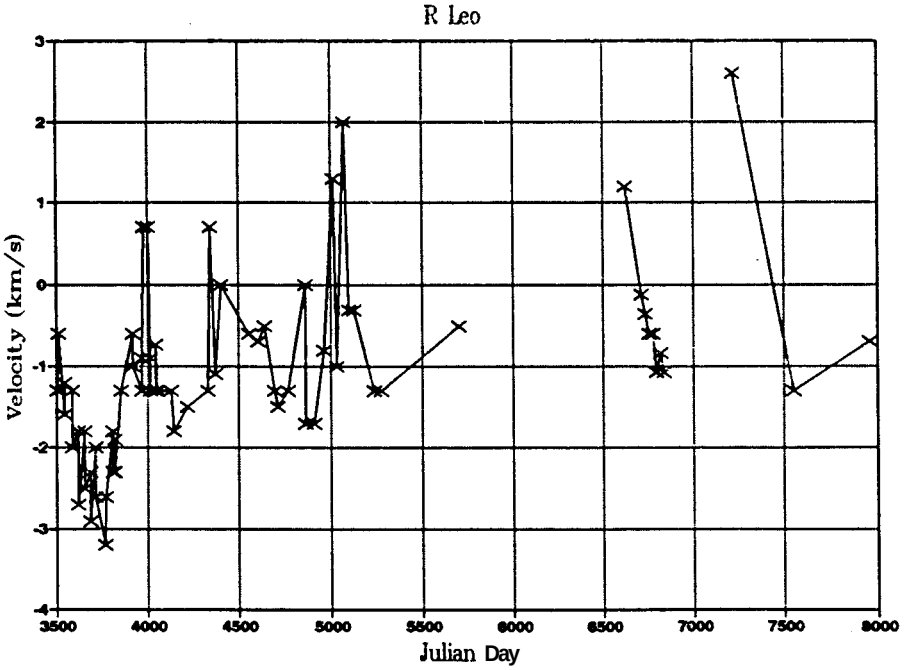

Figure 12: Variation of velocity over very large time-scales, to check Curtis-Struck Marcell (1988)'s model

0.11 km/s. The order of velocity shift observed between the lines from different v states is typically about 1 to 2 km/s, the higher v state line having a higher velocity. In some sources there is no velocity shift, while in three sources, V Cam, VY CMa and S CrB, the difference between the v=2 velocity and the v=1, is greater than ~ 4 km/s. Alcolea et al. (1989) find that the maxima and minima for the v=1,2 and 3 lines occur at the same epoch but the strength of the v=3 emission is not related to the strengths of v=1 and v=2 lines, at the same epoch. Later we shall see that v=3 emission is likely to be unsaturated.

As we shall see, the velocity differences between the $J = 1 \rightarrow 0$ transitions in different v states are consistent with these masing regions being in the close neigbourhood of each other, within about 1–2 x 10^{13} cms.

7.3 SiO maser theory

Soon after the discovery of the circumstellar SiO maser, a theory for population inversion was given by Kwan and Scoville(1974). This model requires the following two assumptions: (1) a large velocity gradient at the location of the maser and (2) large optical depth in the vibrational transition from the vibrational level containing the inverted rotational levels, to the one immediately lower. Under these assumptions, the rate of depopulation turns out. to be independent of the dipole moment for every rotational level in the upper vibrational state. For any level say vibrational state v=1, this rate is given by $\dot{N} = -(A/\tau)N$, where A is Einstein's coefficient for v=1 to v=0, and τ is the optical depth at the corresponding frequency and N is the population in the level. This expression comes from the usual rate equations (ignoring all collisional processes to and from these levels), and using the Sobolev approximation which replaces the

mean line-averaged specific intensity by the local source function multiplied by $(1-\beta)$, where β is the escape probability. It is a function of the velocity gradient and is given by

$$\beta = \frac{1 - e^{-\tau}}{\tau} \tag{2}$$

when τ is isotropic. Since this rate of depopulation is independent of the molecular dipole moment every rotational level in v=1 state is depleted at the same rate. However, each rotational state has two paths of deexcitation to the rotational levels in the v=0 state (as per the selection rule $\mathbf{AJ} = \pm 1$), and a degeneracy of (2J+1). Therefore, the depopulation rate per *substate* is proportional to $2/(2J+1)$, leading to more deexcitation per second for lower J values and hence a population inversion.

Kwan and Scoville had ignored the collisional transitions in calculating the depopulation rate. Later several authors have included the effect of collisions in their numerical calculation of the level populations. Indeed, the population inversion depends sensitively on collisional cross-sections (Langer and Watson 1984). How the molecules reach the v=1 state depends on the pump mechanism. Kwan and Scoville assumed it to be radiative excitation to v=2 and higher states from the ground state. All the following papers in the next decade, were basically variations on this theme. This work is summarized by Langer and Watson (1984), who also present an improvement over previous calculations by using more reliable collisional coefficients, a larger number of levels and a more stable numerical method but they fail to explain the maser power of 10^{44} photons sec^{-1} within any acceptable range of parameters describing the atmosphere of a typical mira variable. This value of the maser power however, may be an overestimate as it is computed assuming an isotropic emission (Alcolea et al.

1989). The other aspects of the Langer and Watson paper can be listed as follows.

1. The variation of the calculated maser power is in phase with the stellar pulsation. We have seen in section 7.2.5 that this accords well with observations. In our view this already allows the conclusion that the maser is saturated and radiatively pumped.

2. The strength of the v=1, J=1 — 0 line is predicted to be weaker than the v=1, J=2 — 1, whereas the 43 GHz flux is observed to be more intense than the flux at 86 GHz in many sources (Snyder and Buhl 1977).

3. They have not tried to predict the relative properties of the maser in different vibrational states.

4. In their calculations, the maximum maser power is obtained closer to the star ($\sim 2R_*$), than the location indicated by the VLBI maps.

5. They have considered only one value of the velocity gradient i.e., $\epsilon = d(ln(V))/d(ln(R) = 1$.

   Later, Alcolea et al. (1989) have recalculated the populations including a larger number of levels, a larger range in the atmosphere's parameters, and in particular different values of ϵ.

We notice that in these calculations there is no attempt to check the consistency between parameters suitable for sufficient maser power and the global properties of the Mira atmosphere. One such parameter is the SiO abundance. Without considering its dependence on the effective temperature, as is true of these calculations, one is unable to explain the cut-off in maser emission for

temepratures beyond 3100 K as seen from our observations earlier. A complete theoretical model of the atmospheres of the Mira variables is still unavailable. The latest work in this direction is that by Bowen (1988). In the following, we confront the numerical simulations with this model of the Mira atmosphere.

7.4 The pumping mechanism and the role of dust

Of the three possible pumping mechanisms for the SiO maser, the chemical pump (creation of SiO molecules with a preference for high-J) was shown to be too slow by Clegg et al. (1983). We therefore do not consider it here any further.

For collisions to be effective, the distance of the masers has to be less than $2R_*$, which is ruled out by VLBI observations. The collisional pump at the VLBI indicated location of masers ($3 \sim 4R_*$), is riot likely because the radiative processes can be easily shown to dominate the collisional ones, given the typical densities $\leq 10^{10} cm^{-3}$; (i.e., $A\beta >$ C, see Cahn and Elitzur, 1979 and Alcolea et tl. 1989). If the masers are assumed to be still further out, one would have to nvoke collisional excitations by molecules associated with the dust grains. In ,hat case, the maser would be expected to follow the variation in the kinetic :emperature of the gas associated with the dust. This variation would lag in)hase with respect to the IR from the star, atleast by $\pi/2$ (0.25 Period) as shown)y Goldreich and Scoville (1976). Thus, there would be a phase-lag between the SiO maser variation with respect to the infra-red variation. The SiO maser rarations on the other hand show no phase-lag with respect to the infra-red ight-curves (as seen in Fig. 6), thus ruling out collisional pumping.

This leaves radiative pumping as the only viable mechanism to excite the

higher vibrational states. The downward cascade will leave a population inverted chain of rotational levels as discussed above in the section on *Maser Theory*. The maser chain may not occur however, throughout all the J levels as pointed out by the observations of Clemens and Lane (1983) and Jewell et al. (1987). We could not find any pattern among the existing observations of higher J transitions. In fact, various reported line-ratios are not in agreement (Schwartz et al. 1970). We therefore do not consider this issue.

The ranges of parameters needed to explain the observed maser power in vibrational states upto v=3, as found by Alcolea et al. (1989), assuming a radiative pump as the likely mechanism, can be listed as,

Velocity gradient parameter	$\epsilon = \frac{R}{V}\frac{\partial V}{\partial R} \geq 1 (\sim 3).$
Kinetic temperature	$T_k = 1000 \sim 1500 K.$
Gas density	$n_{H_2} \leq 10^{10} cm^{-3}.$
SiO abundance	$\frac{n_{SiO}}{n_{H_2}} \sim 5 \times 10^{-5}.$
$P = n_{SiO} R/V$	$6 \times 10^{13} cm^{-3} s$

We now attempt to check if these parameters agree with the expected values for a typical Mira variable, at the location of the maser. Obtaining from Bowen (1988), the velocity, temperature and density profiles as a function of radial distance from the star, and time (see Fig. 13), at a distance of $4R_*$ corresponding to the location of the SiO masers, we find the following physical parameters:

Distance to the maser,	$R \approx 6.8 \times 10^{13} cm$
Velocity	7 km/s
Velocity gradient parameter	$\epsilon \sim 4$
Kinetic Temperature of gas	1200 K
Density of gas	$10^{-16}\ gm\ cm^{-3}$ $(3 \times 10^7 cm^{-3})$

These parameters are derived independently of any requirements from SiO masers, and involve minimal assumptions (Bowen, 1988). Therefore, the agree-

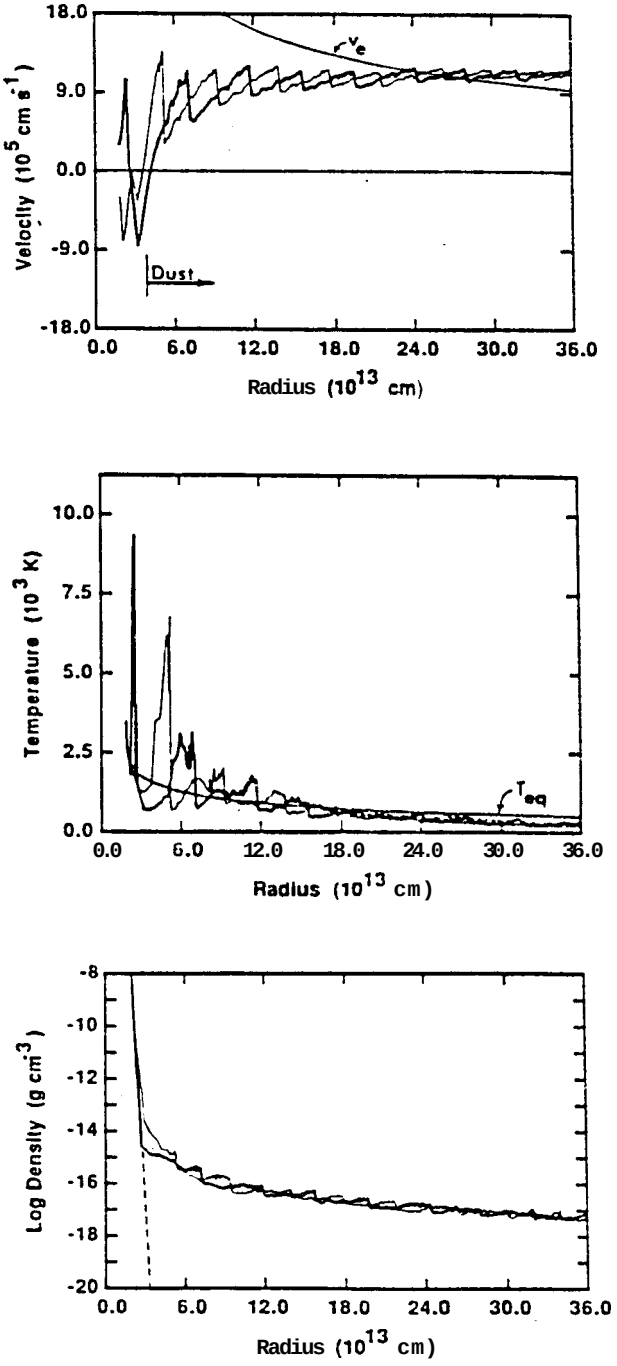

Figure 13: Model atmosphere of a typical Mira variable (Bowen, 1988)

ment of these values with those needed for the operation of the maser, lends further support to the radiative pump mechanism. On the other hand, the additional consistency between the radiative pump picture with the following points discussed earlier, namely,

- Location of the masers as derived from VLBI maps,
- $A\beta > C$ and no phase-lag with respect to IR,
- correlation between maser power and the bolometric luminosity,

indicates that Bowen's derived description of the atmosphere of a typical Mira variable, which is hard to assess observationally, is realistic.

While the values of ϵ, T_k and n_{H_2} are in reasonable agreement between those of Bowen's model and Alcolea et al.'s numerical calculation to produce the observed maser power, at a location for the maser at $\sim 3R_*$, one of the parameters seems to be in disagreement by over or about a factor of 100. This parameter is defined by Alcolea et al., as $\mathrm{P} = n_{SiO}R/V$. For having a sufficient optical depth in the v=1 maser transition, according to Alcolea et al.'s calculations, one needs $\mathrm{P} \sim 6 \times 10^{13} cm^{-3}s$. Whereas, at $3R_*$, Bowen's model shows a value of about 5×10^{11}. The possible error on the individual values of R and V together will give rise to a factor not more than 5 at the most (Bowen, 1988,1989). Increasing the value of R/R_* leads to a decrease in n_{H_2} thus the latitude of variation in P is very small in Bowen's model. The good agreement in other parameters together with this fact, forces us to believe that the value of relative abundance of SiO which has been taken to be $\sim$ 5 x 10^{-5} in previous calculations is an underestimate.

However, an X_{SiO} value of $\sim 10^{-3}$ seems very high, and whether constraints

from the stellar evolution theory would permit it is not clear. For complete consistency, either the Mira atmosphere models should permit larger values of R/V or the numerical calculations of level populations should permit lower values of P.

7.4.1 The pumping constraint

The v=1 and v=2 masers have similar profiles (Alcolea et al. 1989, Allen 1984). Also, as we noted in section 7.2.6, the velocity differences between the J=1—0 transitions in different v states are about 1 km/s. In the framework of Bowen's model, this is consistent with these masing regions being in the close neighbourhood of each other, within about 1–2 10^{13} cms. The nearly thermal line-widths of both these transitions suggest that these are most likely saturated masers. That the time-variation of the maser is in phase with pulsation also indicates this as we have noted earlier. However, v=3 maser profiles are significantly narrower suggesting unsaturation.

For a saturated maser, the following constraint has to hold (Elitzur, 1982),

$$N_m/N_p = \eta < 1, \tag{3}$$

where N_m is the maser photon luminosity, N_p is the pump photon rate and η is the efficiency of the maser. We now check whether the radiative pump satisfies this condition if the pump photons are provided by the star, a black-body emitter at a temperature of 2500 K. Let I_{ν_p} denote the Planckian specific intensity of the star, $\Delta\Omega_*$, the solid angle subtended by the star at the location of the maser, AS be the area offered by the masing region, ν_p be the frequency of the pump photons emitted in the bandwidth of $\Delta\nu_p$ (corresponding to the thermal width

of $\sim$ 1 km/s). Then we have,

$$N_p = \frac{I_{\nu_p} \Delta\Omega_*}{h\nu_p} \Delta\nu_p \Delta S. \tag{4}$$

From the values of Einstein;s coefficients $A_{v'v''}$ for the vibrational transition $v' \rightarrow v''$ (see section 1.2), we know that for pumping the v^{th} level, one has to consider also the excitation from v=0, atleast of the $(v+1)^{th}$ level if not the higher levels; but for temperatures which we shall encounter, even the inclusion of $(v+1)^{th}$ level is not very significant. With

$$\Delta\Omega_* = \frac{\pi R_*^2}{R^2},$$

$$\Delta S = 4\pi R^2, \tag{5}$$

and $R = 3R_*$, we get the following values of N_p, for masers in various v-levels:

Table 2 : Pump rates

photons/s
8.02

Where, F is the area filling factor

$$F = \frac{\Delta S}{4\pi R^2}. \tag{6}$$

On the other hand, the observed maser photon-luminosity varies from 10^{43} to a few $\times 10^{44}$ photons/s as seen from our observations (see Fig. 6.9). From this sample, we see that there are 6 sources whose luminosities exceed the value of 10^{44} photons/s. These sources are: χ Cyg, GX Mon, S Per, VX Sgr, NV Aur and WX PSc. On omitting these sources, we find the mean photon-luminosity to be $\sim 3 \times 10^{43}$ photons/s, which agrees with the values quoted in literature

(Alcolea et al. 1989). The strong SiO sources (as above, and TX Cam, IK Tau etc...) whose luminosities exceed 5 x 10^{43} photons/s, pose a "power problem" as we see below. Now we find from Table 2, that the condition $N_m = \eta N_p$ is satisfied if $\eta F = 0.8$. This implies that both η and F should be > 0.8. For the strong masers mentioned earlier, whose luminosities may exceed 10^{43} photons/s, we already have a shortage of pump photons.

7.4.2 Cut-off in bolometric magnitude

The correlation between maser luminosity and the bolometric magnitude discussed earlier shows that there is no maser power from stars having bolometric magnitudes fainter than -4.8 magnitudes. The total luminosity L. is related to the bolometric magnitude by,

$$L_* = 3.02 \times 10^{35} \times 10^{-\frac{2}{5}M_{bol}} ergs.s^{-1}. \quad (9)$$

Thus the minimum luminosity required for the maser is $2.5 \times 10^{37} ergs.s^{-1}$. For a temperature of 2500 K, this corresponds to a stellar radius of about $3 \times 10^{13} cms$. In the v=0 → v=1 line, with the thermal width of 1 km/s, the photon luminosity from such a black-body is about 4 x 10^{42}. This will further be reduced by a dilution factor, at the location of the maser. This value of luminosity clearly leads to a maser luminosity much smaller than the observed mean. The cut-off in M_{bol} is therefore simply an indication of a weak pump. Perhaps these stars can still show very weak and unsaturated masers.

7.4.3 Radiation from dust

We now estimate an increase in the pump photon rate by including the re-emission from the heated circumstellar dust shell. Previous models have either

not included the dust shell's contribution to the pump radiation or have found it insignificant leading to the proposition that the dust is unimportant as a source of radiation for the pumping of SiO masers (Langer and Watson 1984).

Morris and Alcock (1977) have investigated this in the context of thermal SiO emission. Also, a detailed model of the circumstellar dust-shell, fitting the near and far-IR observations from several Mira variables is now available (Rowan-Robinson ,1983). One of the parameters he derives is the ultra-violet ($\lambda < 0.4\mu$) optical depth of the dust shell, $\tau_{dust}(uv)$. The relative contribution of starlight, scattered light and the emission from dust as a function of wavelength and $\tau_{dust}(uv)$ is seen in Fig. 15 (which is Fig. 4 of Rowan- -Robinson, 1983). In Table 3, we have listed the SiO maser luminosities of some sources from our observations, along with the value of τ_{dust}(uv). We see from this table that the strong SiO maser sources have optical depths greater than 0.5. From Fig. 14 we see that for the wavelengths between 2μ and 10μ, which are relevant for pumping, the contribution from dust is likely to be significant.

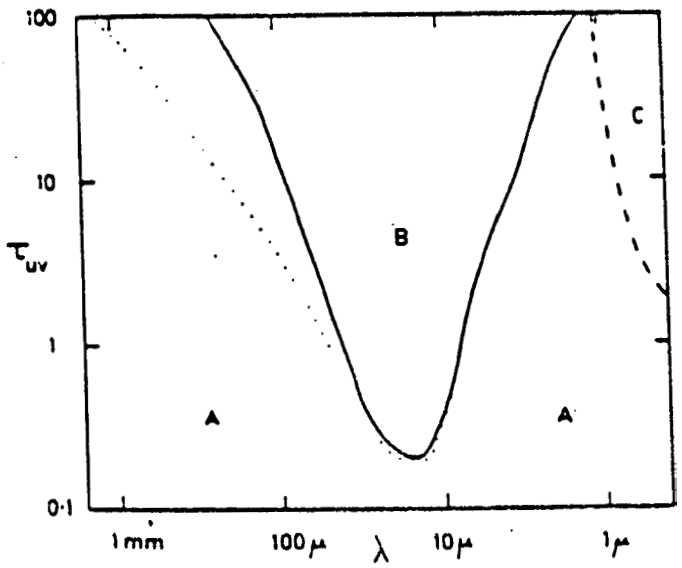

Figure 14: Relative contribution of IR from the star and the circumstellar dust-shell (Rowan-Robinson, 1983)

Table 3: Maser luminosity and Dust optical-depth

Source	SiO 10^{44} Photons S^{-1}	$\tau_{dust}(uv)$
R Aqr	**0.45**	1
RX Boo	**0.024**	0.2
TX Cam	**0.57**	5
o Cet	**0.81**	0.2
R Cnc	**0.23**	0.2
X **Cyg**	**5.92**	2
U Her	**0.49**	0.2
R Hor	**0.05**	0.2
W Hya	**0.52**	0.5
R Leo	**0.25**	0.2
R **LMi**	**0.14**	0.5
S Per	**1.9**	2
VX Sgr	**4.38**	10
IK Tau	**0.59**	5
NV Aur	**2.07**	20
WX Psc	**2.71**	40

As done by Morris and Alcock (1977), we include the effect of the dust on the radiative excitations as follows. We define W„ as the ratio of the dust emission to stellar emission at a given frequency. At the location of the masing region, for an optically thin dust shell,

$$W_\nu = \frac{\tau_d I_\nu(T_d)\Delta\Omega_d}{I_\nu(T_*)\Delta\Omega_*}, \tag{10}$$

where, **I,,** denotes the sum of specific intensities for the two frequencies corresponding to v=0 to v=i and v=0 to v=i+1, for the excitation of v=i level. The solid angle subtended by the dust-shell at the masing region, $\Delta\Omega_d = 4\pi - \mathbf{AR}$, Assuming typical values of T_*=2500 K and T_d=1000 K, we obtain the following values for W,,,for R = $4R_*$,($\Delta\Omega_d = 63 \times \pi/16$)

v	W_ν ($\tau_d = 0.2$)	W_ν ($\tau_d >> 1$)
1	1.54	7.7
2	0.71	3.55
3	0.29	1.45

To include the contribution of the dust to the pump, we thus have to multiply the earlier value of N_p by $(1 + W_\nu)$ obtained from the above table. We see now that the strong maser sources (which have a large value of dust optical depth) will get an enhancement in the pump rate by as much as an order of magnitude. One can also see that for Mira variables having optically thin dust shells, the pump condition is comfortably satisfied and leads to an interesting approximate relation between the efficiency of the maser and the area filling-factor: $\eta F \leq 0.8$. Further, the ratio of v=1 to v=2 maser intensities, which is observed to be close to unity (Alcolea et al. 1989), implies

$$\frac{\eta_1}{\eta_2} \frac{N_p(v=1)(1+W_{\nu 1})}{N_p(v=2)(1+W_{\nu 2})} \approx 1. \qquad (11)$$

We have already seen that both η_1 and η_2 should be larger than 0.8. If the dust contribution is neglected then $\eta_2 > 0.8$ will imply $\eta_1 > 1$. However, if the dust contribution is included, from Table 2 and the above values of A_{Tp} and W_ν, then η_1 and η_2 could be comparable and not exceed unity.

In summary, several independent observational considerations favour the radiative pump for the SiO maser. However, the pump mechanism is severly constrained by the observed maser photon-luminosities, particularly that of some strongly masing Mira variables and supergiants. We have shown that a likely solution to this power shortage may be a significant contribution of pumping radiation from the circumstellar dust-shell.

7.5 Conclusions

The conclusions of this thesis are summarized pictorially in Fig. 15.

We also take this opportunity to list here suggestions for future work.

1. More number of high angular resolution observations of the masing spots are needed, time-monitored VLBI observations will lead to a better understanding of the kinematics of the Mira atmosphere.
2. The detection of SiO maser emission from T Cnc needs to be confirmed. A search for emission from other similar objects will help to check whether these carbon stars have oxygen enriced atmospheres, as seems to be indicated by the IRAS Low Resolution Spectra.
3. Relation between the linear polarization in different components of the line needs to be explored by polarimetric observations.
4. Short term (few hours) time monitoring of the maser emission using a dual polarized receiver will help investigate the effect of the variation of the conditions in the Mira atmosphere on the maser phenomenon.
5. More number of near-simultaneous observations of thermal (v=0) and masing transitions are needed to confirm the anti-correlation between the maser strength and the amplitude of pulsation.
6. Time-monitored observations of the maser flux along with the near IR flux will further confirm radiative pumping. (Particularly in the case of R Hya, where the visual light curve lags the IR).

Figure 15: Summary

REFERENCES

Alcolea J., Bujarrabal V., Gallego J. D., 1989, *Astron. Astrophys.* 211, 187.

Allen B.,1984 Ph.D. Thesis, MIT.

Bertschinger E., Chevalier, R. A., 1985, ***Ap. J.*** 299,167.

Bowen G. H., 1988, ***Ap. J.*** 329,299.

Bowen G. H., 1989, ***"Evolution of Peculiar Red Giants"***, *IAU Coll. **106*** Ed: Johnson H. R., Zuckerman B. (Cambridge Univ. Press)

Cahn J. H., Elitzur M., 1979, ***Ap. J.*** 231,124.

Clark et al., 1984, ***Ap. J.*** 276,572.

Clegg R. E. S., et al., 1983, ***Mon. Not. Royal Astron. Soc.*** 203,125.

Clemens D. P., Lane A. P., 1983, ***Ap. J. Lett.*** **266**,L117.

Curtis Struck-Marcell, 1989, ***Ap. J.*** 330,986.

Elitzur M., 1982, ***Ap. J.*** 262,189.

Engels D., Heske A., 1989, ***Astron. Astrophys. Suppl. Ser.*** 81,323.

Genzel R., et al., 1980, ***Ap. J.*** 239,519.

Goldreich and Scoville 1976 ***Ap. J.*** 205,144.

Harvey et al., 1974 ***Ap. J. Supp. Ser*** 27,331.

Hinkle et al., 1982 ***Ap. J. Supp. Ser*** **56**,1.

Hjalmarson A., Olofsson H., 1979, ***Ap. J.*** **234**,L199.

Jewell P. R., et al., 1987, ***Ap. J.*** 323,749.

Johnson H. R., et al., 1975 ***Ap. J. Supp. Ser.*** 29,123.

Kwan and scoville 1974 ***Ap. J.*** **194**,L97.

Lane A. P., 1984, IAU Symp 110, VLBI and compact radio sources, (D. Reidel Publ. Co.), p 329.

Langer S. H., Watson W. D., 1984, ***Ap. J.*** 284,751.

Lockwood G. R., 1972, ***Ap. J. Suppl. Ser.*** 24,375.

Martinez A., Bujarrablal V., Alcolea J., 1988, ***Astron. Astrophys. Supp. Ser.*** 74,273.

McIntosh G. C.,et al., 1989, ***Ap. J.*** 337,934.

Moran J. M., et al., 1979, *Ap. J.* 231,124.

Morris M., Alcock C., 1977, *Ap. J.* 218,687.

Nyman 1984 Ph. D. Thesis, Chalmers Univ. of Technology.

Plambeck R. L., et al., 1989 Publ. *Astron. Soc. Pac.* 104,879.

Rinsland C. P., Wing R. F., 1982, *Ap. J.* 262,201.

Rowan-Robinson 1983 *Mon. Not. Royal Astron. Soc.* 202,767.

Schwartz *P.* R., et al. 1970, *Ap. J.* **159**,L123.

Snyder L. E., Buhl D., 1975 *Ap. J.* 197,329.

Troland T., et al., 1979, *Ap. J.* 232,143.

Tsuji T., 1978, *Astron. Astrophys.* **62**,29.

Wright *M.* C. H., et al., 1990, *Astron. J.* 99,1299.